Gold Nanocrystals

DOI: 10.1002/anie.200704094

Directed Surface Overgrowth and Morphology Control of Polyhedral Gold Nanocrystals**

Daeha Seo, Choong Il Yoo, Ji Chan Park, Seung Min Park, Seol Ryu, and Hyunjoon Song**

Morphology control of gold nanocrystals has been widely investigated following the first report that the optical properties of nonspherical gold nanoparticles are extremely dependent on their size and shape.[1] In principle, high-symmetry structures can feasibly be generated in a face-centered cubic lattice system when the *R* value, defined as the ratio of relative growth rates along {100} and {111}, is regulated precisely.[2] In the case of silver, poly(vinyl pyrrolidone), PVP, a surface-regulating agent, is proposed to be selectively bound on the {100} faces, and promotes directed growth of planes other than {100} to form silver cubes and nanowires.[3] However, the synthetic methodology for a certain shape is not readily applicable to other structures, because the different faces of the metal nanocrystals are distinguishable only within a narrow range of reaction conditions.[4] Recently, it was found that underpotential deposition (UPD) could account for gold nanorod formation when silver ions are added to the reaction mixture.[5] We also introduced Ag^+ ions to gold polyhedron synthesis and obtained regular shapes from octahedral to cubic in high yields.[6] It is anticipated that such a Au/Ag^+ UPD system can be employed as a general tool for directed growth of {111} faces, whereas addition of Au^{3+} enhances {100} growth to stabilize the entire polyhedral structure. Herein, we applied this directed-growth approach to gold polyhedral seeds and observed complete shape conversion between cubes and octahedra. Recently, similar overgrowth strategies were reported for the synthesis of gold[7] and palladium[8] nanocrystals. We also synthesized cubes, cuboctahedra, and octahedra in high yields from small and large spherical seeds and analyzed their optical properties by discrete dipole approximation (DDA) calculations.

Octahedral and cubic gold seeds were synthesized by a modified polyol process in boiling 1,5-pentanediol (PD), as reported previously.[6] The seed solutions in ethanol were transferred to PD and were set to 0.025 M with respect to the concentration of the gold precursor. For conversion of octahedra to cubes, $AgNO_3$ was added to boiling PD prior to adding the gold precursor. The solution of octahedral seed was introduced, and PVP and $HAuCl_4$ solutions were then added periodically over 7.5 min, followed by refluxing the mixture for 1 h. The scanning electron microscopy (SEM) image in Figure 1b shows uniform octahedral seeds with an

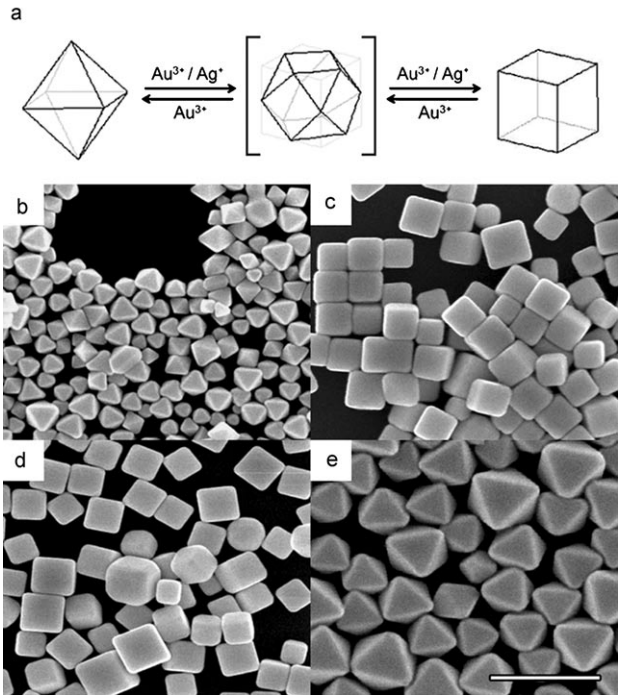

Figure 1. a) Shape conversion between octahedra and cubes. SEM images of b) octahedral seeds, c) cubes grown by addition of Ag^+ and the gold precursor, d) cubic seeds, and e) octahedra grown by addition of the gold precursor without Ag^+. The bar represents 500 nm.

average edge length of 100 nm. As the reaction proceeded, the shape of the seeds changed from octahedral to truncated octahedral, cuboctahedral, and finally perfect cubic (see the Supporting Information). The resulting cubes have relatively sharp edges with an average length of 144 ± 14 nm (Figure 1c), which corresponds to the length of an ideal cube ($\sqrt{2} \times 100$ nm) produced by exclusive {111} surface growth from the original octahedral structure. X-ray diffraction (XRD) data also reveal evolution of the {100} surface from

[*] Prof. S. M. Park, Dr. S. Ryu
Department of Chemistry, Kyung Hee University
Seoul 130-701 (Korea)
Fax: (+82) 2-966-3701
E-mail: sryu@khu.ac.kr
D. Seo, C. I. Yoo, J. C. Park, Prof. H. Song
Department of Chemistry and School of Molecular Science (BK21),
Korea Advanced Institute of Science and Technology
Daejeon 305-701 (Korea)
Fax: (+82) 42-869-2810
E-mail: hsong@kaist.ac.kr

[**] This work was supported by a Korean Research Foundation Grant funded by the Korean Government (MOEHRD, Basic Research Promotion Fund, KRF-2005-205-C00040, to D.S., C.I.Y., J.C.P., and H.S.) and the Korean Science and Engineering Foundation (Grant No. R01-2006-000-10396-0, to S.M.P. and S.R.).

Supporting information for this article is available on the WWW under http://www.angewandte.org or from the author.

the octahedral seeds. For the conversion of cubes to octahedra, the solution of cubic seeds was added to boiling PD, and PVP and $HAuCl_4$ solutions were added periodically over 7.5 min; the mixture was subsequently heated at reflux for 1 h. The new octahedra grown from the original cubes (Figure 1d) have exactly identical structure to the 100-nm-edged octahedra except for the particle size (Figure 1e). The XRD spectrum shows a {111} diffraction peak of very high intensity relative to the other peaks, which reflects the preferred orientation of the octahedral structures normal to the {111} faces. Electron diffraction exhibits a hexagonal pattern, indicative of an exposed surface of {111} with a zone axis of ⟨111⟩ (see the Supporting Information). The average edge length is estimated as 205 ± 15 nm, which is a further indication ($\sqrt{2} \times 140$ nm) of surface overgrowth of {100} faces of the cubic seeds.

It appears that there are two important factors for complete shape conversion of polyhedra by selective surface overgrowth: the presence of Ag^+ and the seed surface structure. $AgNO_3$ has already been reported to be a key element for the synthesis of gold nanostructures.[5,9] The original surface structure also guides crystal growth directions in some cases. Yang et al. reported that GaN nanowires with different growth directions could be produced by changing the single-crystalline substrates.[10] γ-$LiAlO_2$ (100) and MgO (111) substrates resulted in nanowire growth along the orthogonal ⟨1$\bar{1}$0⟩ and ⟨001⟩ directions, respectively, under identical experimental conditions. To determine the major influencing factor for shape conversion, cuboctahedra (Figure 2c) were chosen as seeds in which both {100} and {111} faces are exposed on the surface. Addition of the gold precursor without $AgNO_3$ converted the cuboctahedra to large octahedra (Figure 2b), whereas addition of 1/200 equiv $AgNO_3$ with the gold precursor afforded large cubes with good shape uniformity (Figure 2d). These results indicate that directed surface overgrowth and subsequent shape conversion are not related to the particular shape of the seed, but are entirely dependent on the presence or absence of $AgNO_3$ in the growth solutions.

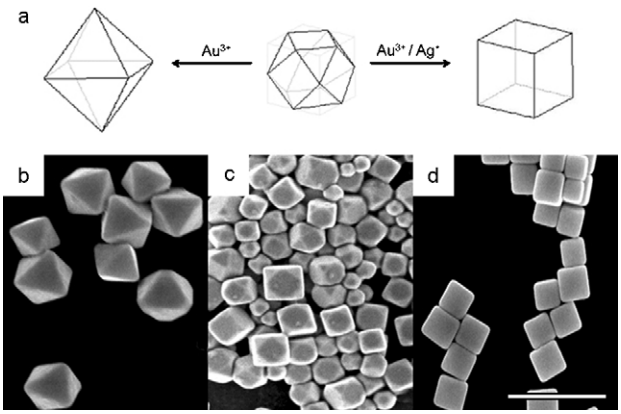

Figure 2. a) Shape evolution of cuboctahedral seeds by changing the growth solutions. SEM images of b) large octahedra grown by addition of the gold precursor, c) cuboctahedral seeds, and d) cubes grown by addition of Ag^+ and the gold precursor. The bar represents 500 nm.

Such complete shape conversion is mainly due to selective underpotential deposition of Ag ions on the gold surface. It is known that the underpotential shift for bulk deposition of a metal onto a different metal substrate is proportional to the difference in work function between the two metals.[11] The Au/Ag^+ system is one of the earliest examples of the UPD phenomena, because the work-function gap of silver and gold is larger than 0.5 eV.[12] The underpotential shift is also sensitive to the distinct surface structures. For Au(100) and (111) planes, the work-function differences with respect to silver are 0.83 and 0.57 eV, respectively, and electrochemical measurements have given underpotential shifts of 0.24 and 0.07 V, respectively.[13] Theoretical calculations on the Au/Ag^+ system also demonstrate selective island growth of Ag on Au(100) but not on Au(111) at intermediate deposition rates.[14] Selective deposition of Ag ions onto the side walls of gold nanorods was observed experimentally.[5,15] Similar behavior may occur under our experimental conditions. Ag^0 reduced from Ag^+ was preferentially deposited onto the {100} seed surface to form silver layers, which suppressed epitaxial overgrowth of the gold layers during the reaction. It is suggested that the reductive environment of PVP and PD at boiling temperature provided appropriate conditions for selective deposition of Ag on the gold surface. Consequently, the growth rate of {100} faces and the R value decreased significantly, and this led to complete conversion of octahedral shapes ($R = 1.73$) to cuboctahedral ($R = 0.87$) and cubic ($R = 0.58$) shapes.[2]

In the absence of silver ions, addition of gold precursor enhances {100} growth to increase the surface fraction of {111} faces. In the face-centered cubic lattice, the relative surface energies are in the order of $\gamma_{111} < \gamma_{100} < \gamma_{110}$ among the lowest index planes, due to the surface-atom density and coordination number with neighboring atoms.[2,4] Therefore, it is apparent that the polyhedral faces tend to form {111} planes on their surface. As a result, cubic seeds (only {100} faces on the surface) are completely converted to cuboctahedra (mixture of {100} and {111}) and octahedra (only {111} faces).

We applied this directed overgrowth approach to control both size and shape of gold nanocrystals. Spherical gold nanoparticles containing 0.02 equiv of silver with respect to gold content were chosen as a starting seed structure. Growth of large spherical seeds (average diameter of 81 ± 8 nm, Figure 3b) generated cubes (average edge length of 116 ± 11 nm, Figure 3d), cuboctahedra (122 ± 13 nm, Figure 3f), and octahedra (236 ± 19 nm, Figure 3h) with increasing amounts of the gold precursor, from 1 to 6 and 12 equiv of the original gold content used for the seed synthesis. On the other hand, when small spherical particles with a diameter of 49 ± 5 nm (Figure 3c) were used as seeds, polyhedra having diameters less than half those of the large particles were produced. The average edge lengths of the smaller particles are 67 ± 6 nm for cubes (Figure 3e), 54 ± 8 nm for cuboctahedra (Figure 3g), and 88 ± 10 nm for octahedra (Figure 3i). All particles have regular polyhedral shapes with narrow size distributions (< 10%). In comparison with a previous synthetic approach to gold polyhedra,[6] this seed-mediated

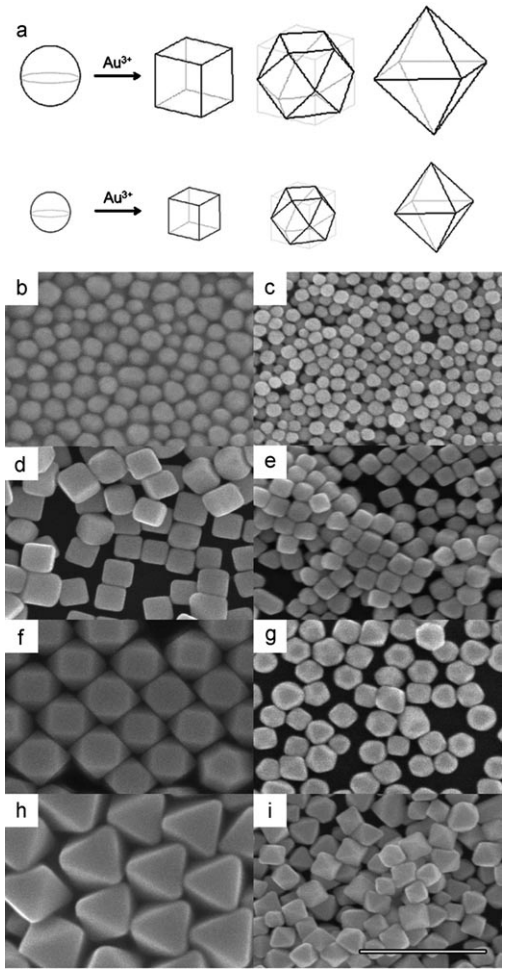

Figure 3. a) Size and shape control of gold polyhedral nanocrystals from spherical seeds. SEM images of b, c) spherical seeds (average diameters: 81 ± 8 and 49 ± 5 nm), d, e) cubes (average edge lengths: 116 ± 11 and 67 ± 6 nm), f, g) cuboctahedra (122 ± 13 and 54 ± 8 nm), and h, i) octahedra (236 ± 19 and 88 ± 10 nm). The bar represents 500 nm.

overgrowth method gave uniform polyhedra in very high yields with small amounts of small self-seeded particles, which were easily removable by centrifugation. Another advantage of this process is that the size of each polyhedral shape can be precisely tuned by using different-sized seeds. Spherical particles have been synthesized with wide size ranges by many processes.[16]

The optical properties of the gold nanocrystals are very sensitive to their size and shape.[17] The UV/Vis extinction of each type of polyhedra was measured and simulated by DDA calculations,[18] which approximate a nanoparticle as a collection of induced dipoles in a small unit interacting with each other and incident light. Using the DDSCAT code developed by Draine and Flatau,[19] we calculated the extinction cross section C_{ext} for each structure at a given wavelength of incident light. The extinction spectrum was averaged rotationally over 320 orientations of the nanoparticle relative to the direction of incident light. The dielectric medium (solvent) was chosen to be water, and the wavelength of the incident light was varied in intervals of 10 nm. The dielectric function of gold was taken from the literature,[20] and the built-in dielectric function of liquid water in DDSCAT[19] was utilized for the medium.

For DDA calculations, we modeled eight three-dimensional shapes of O_h symmetry using point dipoles in the cubic lattice, reflecting SEM observations that small portions of the edges or apices of nanoparticles are rounded off. Sufficient numbers of point dipoles construct polyhedral structures, and thus the simulated extinction properties show minimal changes with respect to any further increase in number of dipoles. A large octahedron having an edge length of 236 nm was constructed with 102331 point dipoles after the six apices were snipped by 12 nm, that is, cut off at the plane perpendicular to the pointing direction of each apex. Likewise, a small octahedron of edge length 88 nm is comprised of 11485 point dipoles after 6-nm snipping. For cubes having edge lengths of 116 and 67 nm, the twelve edges are sliced off by 8 nm at the plane perpendicular to the line representing the shortest distance from the center of mass to an edge, so that 27807 and 10759 point dipoles represent the structures, respectively. For cuboctahedra, we did not apply any snipping or edge cutting, because the ideal structure has very obtuse angles at apices and edges and a rounded-off structure is not visible in SEM images, in contrast to cubes and octahedra. Thus, 122- and 54-nm-edged cuboctahedra consist of 67187 and 19909 dipoles, respectively. Lastly, 33552 and 18853 point dipoles were used for spheres of 81 and 49 nm diameter, respectively.

Extinction spectra for small and large spheres show single sharp peaks at wavelengths of 525 and 560 nm (Figure 4a), which DDA and Mie calculations[21] assign to dipolar plasmon resonances. In the case of cubes, we found that the small cube structure (with an effective radius of 39.9 nm) has roughly the same volume as a large sphere (radius 40.5 nm), but the peak appears at 570 nm (Figure 4b), which is red-shifted by about 10 nm from that of the large sphere. The large cube, on the other hand, exhibits two peaks in the optical range in which the long-wavelength and short-wavelength peaks correspond to dipolar and quadrupolar plasmonic resonances (Figure 4b). Comparison with the Mie calculation verifies that the overall spectral shape is similar to the extinction spectrum of a sphere of the same volume but red-shifted by 50 nm.

The same argument can be employed for the spectra of cuboctahedral structures. Since the critical radius of a gold particle that can exhibit quadrupolar and dipolar resonance is about 65 nm according to Mie calculation,[21] the small cuboctahedron (effective radius 49 nm) shows only a dipolar peak at 580 nm, while the large cuboctahedron (effective radius 101 nm) shows dipolar and quadrupolar peaks at 800 and 580 nm (Figure 4c). The small octahedron (effective radius 42.5 nm) shows only a dipolar peak at 595 nm, while the large octahedron exhibits three peaks, at 1000, 760, and 570 nm (Figure 4d). For the latter, the weakest peak near 1000 nm corresponds to dipolar resonances from edge and cross modes, which are practically inseparable, as reported for smaller octahedral structures.[22] Unlike dipolar resonances, however, the quadrupolar peak from an edge mode of gold octahedra with edge lengths exceeding 150 nm is well separated from the other quadrupoles. The strongest peak,

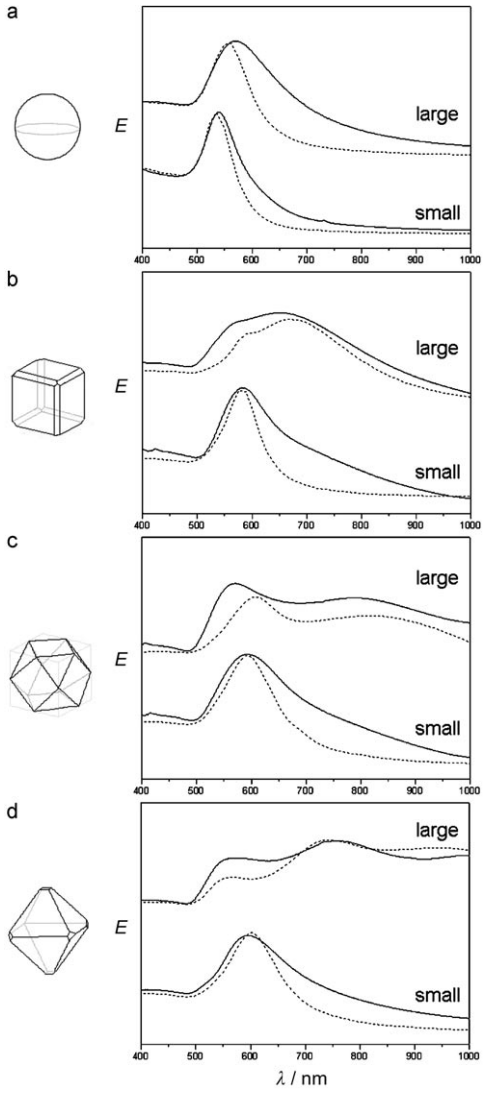

Figure 4. UV/Vis extinction spectra (solid lines) and results of DDA calculations (dotted lines) of a) large (diameter 81 nm) and small (49 nm) spherical seeds, b) large (edge length 116 nm) and small (67 nm) cubes, c) large (edge length 122 nm) and small (54 nm) cuboctahedra, and d) large (edge length 236 nm) and small (88 nm) octahedra.

at 760 nm, is assignable to an edge quadrupole, whereas the 570-nm peak originates from a cross-quadrupolar excitation with a small contribution of an edge octupole (Supporting Information).

The optical spectra of eight different nanoparticles are summarized as follows: First, small particles having radii less than about 65 nm show a single dipolar peak in the 500–600 nm range, and peak positions are red-shifted as the particle shape is modulated and deviates from a sphere with the same volume. Second, large particles exhibit two or more peaks in the optical range due to higher multipole excitations, and their positions are also red-shifted from the peak positions of a sphere of identical character with the same volume, consistent with optical responses of large metal particles.[23]

In conclusion, we have controlled the shape and size of gold polyhedra simultaneously by directed surface overgrowth from polyhedral and spherical seeds. The resulting cubes, cuboctahedra, and octahedra exhibit characteristic optical properties in the visible range, which could be analyzed by DDA calculations. The variation of UV/Vis extinction in gold polyhedral nanocrystals is applicable to sensors and wave guides based on surface plasmon resonance. It is also anticipated that a similar directed-overgrowth approach would provide various nanocrystal structures in other face-centered cubic systems, such as palladium, platinum, rhodium, and iridium, which are promising catalysts for surface-dependent chemical reactions.

Experimental Section

Shape conversion: Octahedral and cubic seeds were synthesized according to literature methods.[6] For conversion of octahedra to cubes, a solution of $AgNO_3$ (0.15 mL, 0.005 M, 99 + %, Aldrich) in 1,5-pentanediol (PD, 96%, Aldrich) was added to boiling PD (5.0 mL). A solution of gold octahedral seeds in PD (1.0 mL, 0.025 M with respect to the gold precursor concentration) was introduced immediately, and then PVP (total 3.0 mL, 0.15 M, $M_w = 55000$, Aldrich) and $HAuCl_4$ (total 3.0 mL, 0.050 M, 99.9 + %, Aldrich) solutions in PD were added periodically every 30 s over 7.5 min. The resulting mixture was heated at reflux for 1 h. For conversion of cubes to octahedra, the solution of gold cube in PD (1.0 mL, 0.025 M with respect to the gold precursor concentration) was added to boiling PD (5.0 mL). PVP (3.0 mL, 0.125 M) and $HAuCl_4$ (3.0 mL, 0.033 M) solutions in PD were added every 30 s over 7.5 min. The resulting mixture was heated at reflux for 1 h. The products were washed with ethanol (99.9%, J.T. Baker) in a repetitive dispersion/precipitation cycle.

Synthesis of spherical seeds: For large seeds (81-nm diameter), $AgNO_3$ in PD (0.15 mL, 0.020 M) was added to boiling PD (5.0 mL). PVP (3.0 mL, 0.15 M) and $HAuCl_4$ (3.0 mL, 0.050 M) solutions in PD were then added periodically every 30 s over 7.5 min. The resulting solution was heated at reflux for 1 h. After purification by centrifugation, the seeds were dispersed in PD (25 mL). For small seeds (49 nm), a solution of $AgNO_3$ (0.15 mL, 0.020 M) in PD was added to boiling PD (11.0 mL). PVP (6.0 mL, 0.25 M) and $HAuCl_4$ (3.0 mL, 0.050 M) solutions in PD were then added periodically every 30 s over 7.5 min. The resulting solution was heated at reflux for 1 h. After purification by centrifugation, the seeds were dispersed in PD (100 mL).

Synthesis of large polyhedra: PVP (3.0 mL) and $HAuCl_4$ (3.0 mL) solutions in PD were added periodically every 30 s over 7.5 min to the solution of large spherical seeds in PD (5.0 mL). The concentrations of PVP and $HAuCl_4$ solutions were 0.050 M and 0.010 M for cubes, 0.18 M and 0.050 M for cuboctahedra, and 0.36 M and 0.11 M for octahedra. The resulting mixtures were heated at reflux for 1 h. All nanocrystals were washed with ethanol several times in a repetitive dispersion/precipitation cycle.

Synthesis of small polyhedra: PVP (3.0 mL) and $HAuCl_4$ (3.0 mL) solutions in PD were added periodically every 30 s over 7.5 min to the solution of small spherical seeds in PD (5.0 mL). The concentrations of PVP and $HAuCl_4$ solutions were 0.027 M and 0.0065 M for cubes, 0.045 M and 0.013 M for cuboctahedra, and 0.090 M and 0.028 M for octahedra. The resulting mixtures were heated at reflux for 1 h. All nanocrystals were washed with ethanol several times in a repetitive dispersion/precipitation cycle.

Received: September 5, 2007
Revised: October 4, 2007

Keywords: crystal growth · gold · morphology control · nanostructures · surface plasmon resonance

[1] a) Y. Xia, N. J. Halas, *Mater. Res. Soc. Bull.* **2005**, *30*, 338 – 348; b) K. L. Kelly, E. Coronado, L. L. Zhao, G. C. Schatz, *J. Phys. Chem. B* **2003**, *107*, 668 – 677; c) J. J. Mock, M. Barbic, D. R. Smith, D. A. Schultz, S. Schultz, *J. Chem. Phys.* **2002**, *116*, 6755 – 6759.

[2] Z. L. Wang, *J. Phys. Chem. B* **2000**, *104*, 1153 – 1175.

[3] a) Y. Sun, Y. Xia, *Science* **2002**, *298*, 2176 – 2179; b) A. Tao, P. Sinsermsuksakul, P. Yang, *Angew. Chem.* **2006**, *118*, 4713 – 4717; *Angew. Chem. Int. Ed.* **2006**, *45*, 4597 – 4601; c) Y. Sun, B. Mayers, T. Herricks, Y. Xia, *Nano Lett.* **2003**, *3*, 955 – 960.

[4] B. Wiley, Y. Sun, B. Mayers, Y. Xia, *Chem. Eur. J.* **2005**, *11*, 454 – 463.

[5] M. Liu, P. Guyot-Sionnest, *J. Phys. Chem. B* **2005**, *109*, 22192 – 22200.

[6] D. Seo, J. C. Park, H. Song, *J. Am. Chem. Soc.* **2006**, *128*, 14863 – 14870.

[7] A. Sánchez-Iglesias, I. Pastoriza-Santos, J. Pérez-Juste, B. Rodríguez-González, F. J. García de Abajo, L. M. Liz-Marzán, *Adv. Mater.* **2006**, *18*, 2529 – 2534.

[8] S. E. Habas, H. Lee, V. Radmilovic, G. A. Somorjai, P. Yang, *Nat. Mater.* **2007**, *6*, 692 – 697.

[9] a) C. J. Murphy, T. K. Sau, A. M. Gole, C. J. Orendorff, J. Gao, L. Gou, S. E. Hunyadi, T. Li, *J. Phys. Chem. B* **2005**, *109*, 13857 – 13870; b) F. Kim, S. Connor, H. Song, T. Kuykendall, P. Yang, *Angew. Chem.* **2004**, *116*, 3759 – 3763; *Angew. Chem. Int. Ed.* **2004**, *43*, 3673 – 3677; c) F. Kim, J. H. Song, P. Yang, *J. Am. Chem. Soc.* **2002**, *124*, 14316 – 14317.

[10] T. Kuykendall, P. J. Pauzauskie, Y. Zhang, J. Goldberger, D. Sirbuly, J. Denlinger, P. Yang, *Nat. Mater.* **2004**, *3*, 524 – 528.

[11] E. Herrero, L. J. Buller, H. D. Abruna, *Chem. Rev.* **2001**, *101*, 1897 – 1930.

[12] L. B. Rogers, D. P. Krause, J. C. Griess, Jr., D. B. Ehrlinger, *J. Electrochem. Soc.* **1949**, *95*, 33 – 46.

[13] a) N. Ikemiya, K. Yamada, S. Hara, *Surf. Sci.* **1996**, *348*, 253 – 260; b) K. Ogaki, K. Itaya, *Electrochim. Acta* **1995**, *40*, 1249 – 1257.

[14] a) M. C. Giménez, M. G. Del Pópolo, E. P. M. Leiva, S. G. García, D. R. Salinas, C. E. Mayer, W. J. Lorenz, *J. Electrochem. Soc.* **2002**, *149*, E109-E116; b) S. Garcia, D. Salinas, C. Mayer, E. Schmidt, G. Staikov, W. J. Lorenz, *Electrochim. Acta* **1998**, *43*, 3007 – 3019.

[15] M. Grzelczak, J. Pérez-Juste, B. Rodríguez-González, L. M. Liz-Marzán, *J. Mater. Chem.* **2006**, *16*, 3946 – 3951.

[16] M.-C. Daniel, D. Astruc, *Chem. Rev.* **2004**, *104*, 293 – 346, and references therein.

[17] a) L. M. Liz-Marzán, *Langmuir* **2006**, *22*, 32 – 41; b) M. A. El-Sayed, *Acc. Chem. Res.* **2001**, *34*, 257 – 264.

[18] a) W.-H. Yang, G. C. Schatz, R. P. Van Duyne, *J. Chem. Phys.* **1995**, *103*, 869 – 875; b) B. T. Draine, P. J. Flatau, *J. Opt. Soc. Am. A* **1994**, *11*, 1491 – 1499.

[19] B. T. Draine, P. J. Flatau, Program DDSCAT, Scripps Institute of Oceanography, University of California, San Diego.

[20] P. B. Johnson, R. W. Christy, *Phys. Rev. B* **1972**, *6*, 4370 – 4379.

[21] a) G. Mie, *Ann. Phys.* **1908**, *25*, 377 – 445; b) C. F. Bohren, D. R. Huffman, *Absorption and Scattering of Light by Small Particles*, Wiley, New York, **1983**, pp. 477 – 482.

[22] C. Li, K. L. Shuford, Q.-H. Park, W. Cai, Y. Li, E. J. Lee, S. O. Cho, *Angew. Chem.* **2007**, *119*, 3328 – 3332; *Angew. Chem. Int. Ed.* **2007**, *46*, 3264 – 3268.

[23] a) I. Pastoriza-Santos, A. Sánchez-Iglesias, F. J. García de Abajo, L. M. Liz-Marzán, *Adv. Funct. Mater.* **2007**, *17*, 1443 – 1450; b) A. S. Kumbhar, M. K. Kinnan, G. Chumanov, *J. Am. Chem. Soc.* **2005**, *127*, 12444 – 12445.

